High Sensitivity Detection of Partial Discharge Acoustic Emission within Power Transformer by Sagnac Fiber Optic Sensor

Sen Qian, Hao Chen and **Yang Xu**
State Key Laboratory of Electrical Insulation and Power Equipment
Xi'an Jiaotong University
Xi'an 710049, China

Lei Su
School of Engineering and Materials Science
Queen Mary University of London
London E1 4NS, UK

ABSTRACT

Partial discharge acoustic detection is an important monitoring tool for power transformer diagnosis, which was traditionally performed by mounting the piezoelectric transducers on the oil tank surface. The disadvantage of partial discharge acoustic detection is its low sensitivity when partial discharge occurs inside the winding, which greatly compromises the value of partial discharge acoustic detection. Fiber optic sensors that can be deployed within power transformer are expected to be a potential solution. In this research, we used a Sagnac fiber sensor system built in lab to investigate the benefits of using fiber optic sensor for partial discharge acoustic detection. Acoustic pulses were induced in oil outside the winding and in oil duct inside the winding of a single phase 50 kV transformer. Although both fiber optic sensor and piezoelectric sensor can effectively detect the acoustic pulses outside the winding, fiber optic sensor gained a much better sensitivity over piezoelectric transducer to detect the acoustic pulses originated inside the winding. We envisage that the proposed fiber sensor can be deployed in power transformers to significantly enhance the detection performance of acoustic emission induced by partial discharge.

Index Terms - **Optical fiber transducers, partial discharges, acoustic transducers, power transformers**

1 INTRODUCTION

POWER transformer as a key component in power grid needs to be monitored to assure its reliability. Among various kinds of monitoring methods, partial discharge (PD) detection is a popular and effective method for power transformer health assessment [1, 2]. When partial discharge occurs, the electromagnetic signal can be picked up by electric sensors such as capacitive couplers or ultrahigh frequency couplers [3]. Although electric sensors were commonly used on site, they were vulnerable to electromagnetic interference that was quite common in high voltage power station.

Various ways have been proposed to overcome the noise interfering with the PD signal, such as wavelet analysis and neural networks [4-6]. However, these methods are only effective in limited scenarios since the denoised pulses collected by online PD monitor are difficult to be confirmed as real PD pulses. Another commonly used method is PD acoustic detection. PD acoustic detection can be used to assist PD electric detection in order to distinguish the noise interference and the PD signal, or in some scenarios where acoustic detection is preferred than electric detection [7]. Previously piezoelectric transducers (PZT) mounted on the surface of the transformer oil tank were commonly used to detect PD acoustic emission. Not only was it able to detect PD, it also helped the professionals determine the PD location [8, 9]. However, the acoustic detection of PD in power transformer was traditionally considered relatively less sensitive. It is illustrated that the acoustic emission from PD inside the winding or between the winding and the core can be hardly detected because of the signal attenuation [7]. This drawback significantly compromises the usefulness of PD acoustic detection because approximately half the faults of power transformer occurred at windings

Manuscript received on 27 October 2017, in final form 5 July 2018, accepted 6 July 2018. Corresponding author: Y. Xu.

according to [10].

Recent developments of fiber optic sensor technology hold the promise of confronting this challenge in PD acoustic detection. Fiber optic sensors (OFS), as insulating dielectric, can be deployed within the power transformer so that the sensor is close to PD source. The closeness to PD source is expected to improve the sensor performance because of less signal attenuation before the acoustic arrives at the sensor. Various fiber optic sensors have been studied in partial discharge acoustic detection. The most widely investigated fiber sensors were interferometers, such as Mach Zehnder interferometer [11-13], Sagnac interferometer [14,15], Michelson interferometer [16], and Fabry Perot interferometer [17,18]. Besides, fiber couplers [19], fiber Bragg gratings [20,21], and optical time domain reflectometry [22] were proposed.

Previous studies primarily were focused on the proof-of-concept experiment of fiber optic sensors in partial discharge acoustic detection. In this research, we first configured a Sagnac fiber optic sensor because it was suitable for detection of high frequency acoustic wave. Then, we used a 50 kV single phase power transformer to investigate the benefits obtained from using Sagnac fiber sensor system deployed within power transformer in comparison to the piezoelectric transducer mounted on the outside oil tank. Our result demonstrates that the embedded fiber optic sensor has a better sensitivity to detect the acoustic wave originated inside the winding, which can effectively enhance the detection performance of partial discharge acoustic emission.

2 CONFIGURATION AND CHARACTERIZATION OF SAGNAC FIBER SENSOR SYSTEM

Schematic diagram of the Sagnac fiber sensor system is shown in Figure 1a, which consists of a 1550 nm light source, a fiber coupler, and an InGaAs photodetector.

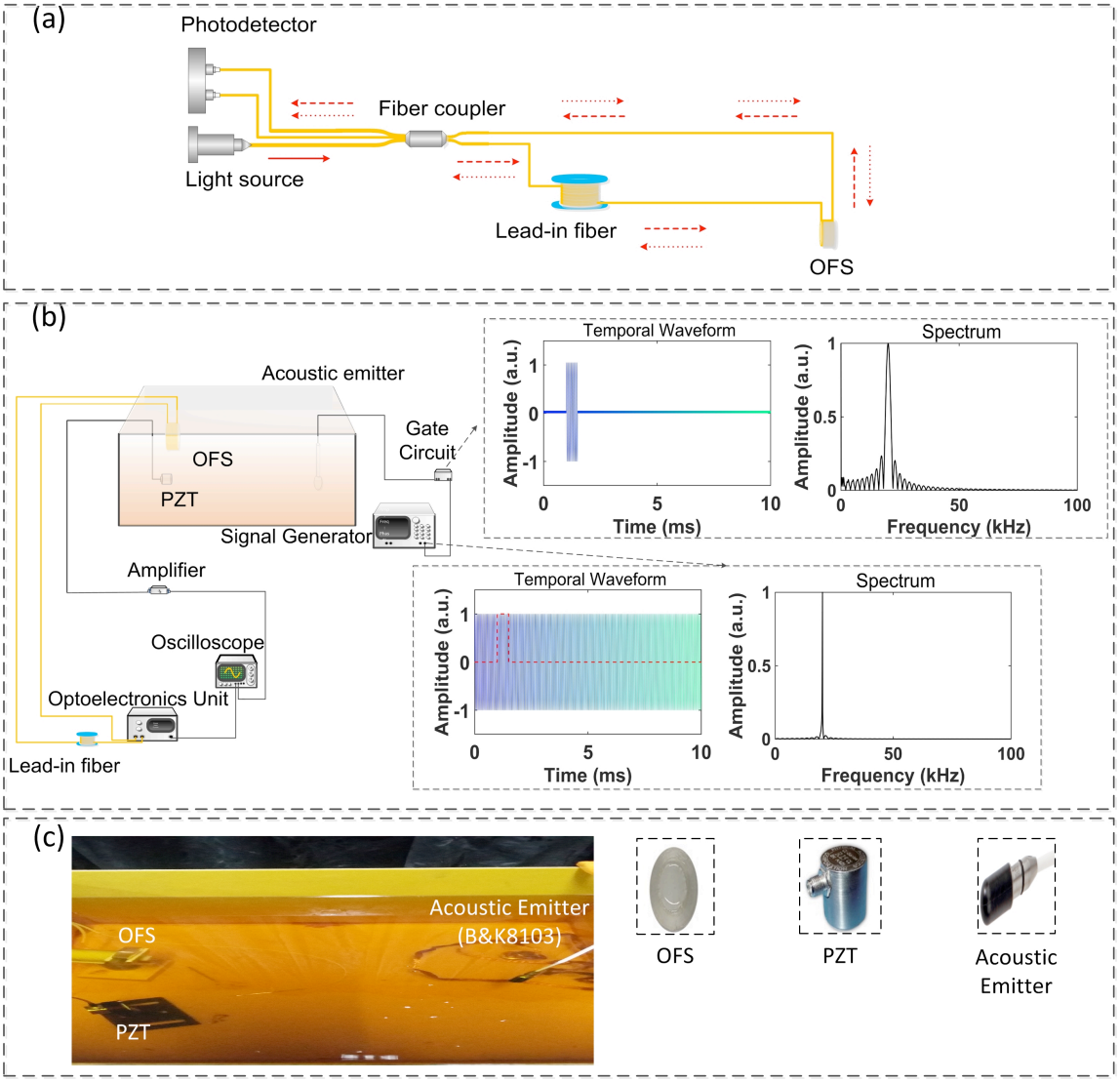

Figure 1. Schematic of Sagnac fiber interferometer and experimental layout; (a) schematic of Sagnac fiber interferometer, (b) schematic of experimental layout, (c) photo of experimental layout.

Light input from the light source was split by the fiber coupler to two waves propagating clockwise, as shown in dotted red arrow, and counterclockwise, as shown in dashed red arrow. After these two waves finish their trips along the fiber loop, they interfere with each other at the photodetector, so the final output can be expressed as,

$$I_{out} = (E_{cw}^2 + E_{ccw}^2) + 2|E_{cw}||E_{ccw}|\cos(\Delta\phi + \Delta\phi_a(t)) \quad (1)$$

where E_{cw} and E_{ccw} are the light fields propagating clockwise and counterclockwise, $\Delta\Phi$ is the phase difference between the clockwise and counterclockwise waves, $\Delta\Phi_a(t)$ is the time varying phase term induced by acoustic perturbation that acts on the OFS. A balanced photodetector that can prevent signal fading and balance out the common mode noise transformed the optical signal to electric signal.

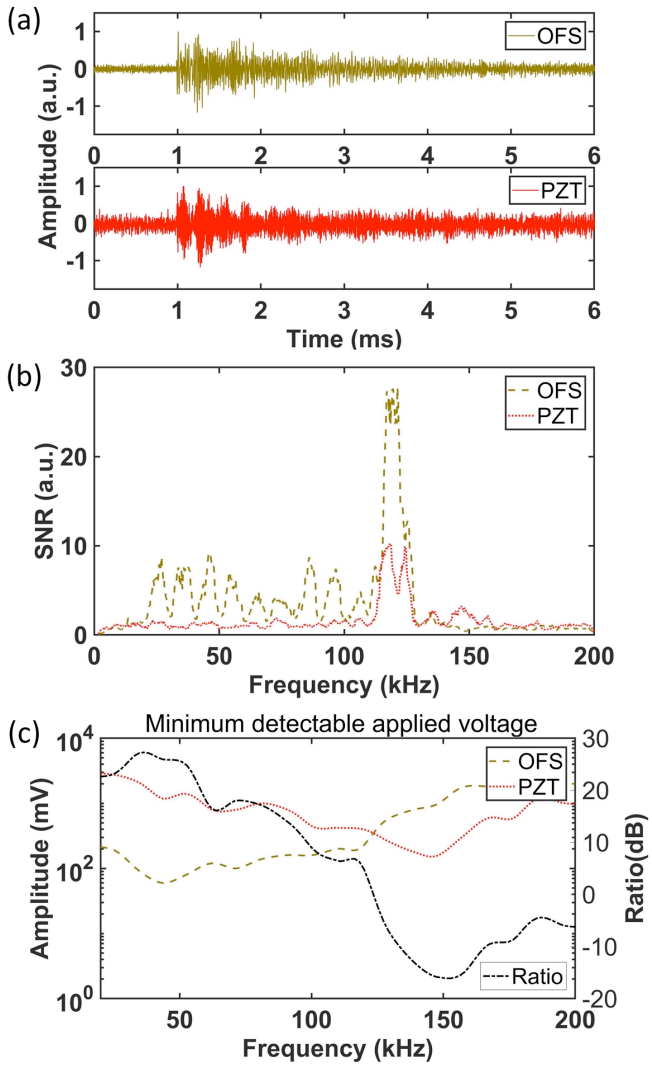

Figure 2. Characterization result of OFS and PZT; (a) temporal waveforms of OFS and PZT when 120 kHz acoustic tone burst was emitted, (b) corresponding power spectral density of signal relative to noise, (c) the minimum detectable applied voltage of OFS and PZT.

The schematic diagram of experimental layout is shown in Figure 1b, where the OFS， PZT and acoustic emitter were placed within an oil tank of 42 cm in length, 42 cm in width, and 33 cm in height which was filled with soybean vegetable insulating oil, with the photo shown in Figure 1c. The light source, photodetector and their driving electronics were encapsulated in the optoelectronics unit. The commercial off-the-shelf PZT, i.e. R15α Physical Acoustic Corporation, was used as the benchmark for comparison. Because the PD acoustic signal generally lies in a broad range of frequency spectrum [23], tone burst was used to simulate the PD acoustic emission [24]. As an example in Figure 1b, the signal generator outputs a 20 kHz sine wave, whose spectrum concentrates on the 20 kHz component. A gate circuit that outputs a rectangle window chops the sine wave to produce a tone burst, whereupon its spectrum is broadened, while the power still concentrates on 20 kHz. Sine waves of 20 kHz ~ 200 kHz gated by window of 100 μs width and 20 ms interval were applied onto the acoustic emitter (AE), i.e. Bruel and Kjaer 8103, to emit the corresponding acoustic tone bursts. The distances between acoustic emitter and OFS and PZT sensor were 36 cm.

An excerpt of detected waveforms when the acoustic emitter was excited by a 1 V 120 kHz tone burst is shown in Figure 2a. The amplitude of the signal to noise level of OFS is higher than that of PZT. Figure 2b shows that power spectral density of the signal to noise ratio (SNR) of OFS is three times that of PZT. The minimum detectable applied voltage, i.e. the applied voltage onto acoustic emitter when the sensors detected a signal of amplitude twice the noise level, is shown in Figure 2c. The black dot dash line indicates the sensitivity gain of OFS relative to PZT expressed in decibel. Ratio above 0 dB means OFS performed better than PZT. It can be seen that the OFS performed better at frequency span from 20 kHz ~ 130 kHz whereas the PZT performed better at frequency span from 130 kHz ~ 200 kHz.

3 PD ACOUSTIC DETECTION EFFICIENCY AT DIFFERENT LOCATIONS

A 50 kV single phase transformer of 960 mm in length, 820 mm in width and 1018 mm in height was used as the model. The PZT was mounted on the outside surface tank by a magnetic clamp, shown in Figure 3b. Acoustic couplant was scrabbled on the outside surface of the oil tank in order to improve the acoustic coupling efficiency. The OFS was deployed on top of the winding. A capacitive coupling unit (LDM-5, Doble Engineering) was used to collect the electric signal as the reference. PD was induced at the tip of needle to cylinder model of 5 mm gap distance. The needle of 1 mm diameter and 5 μm radius was made of stainless steel. The lower cylinder was made by wrapping the copper foil onto the copper wire, as shown in the inset in Figure 3b. The winding consisted of 5 layers, with 8 cm total width. The width of the oil duct was 1 cm.

The PD source was placed in oil outside the winding, as shown in Figure 4a. The distances from the PD source to the OFS and PZT were approximately 15 cm. The voltage was increased to 8 kV when all the three sensors captured the PD pulses. An excerpt of the captured waveforms during a single power cycle is shown in Figure 4b, where two pulses were

detected by LDM-5, OFS and PZT. The waveform of PZT showed two pulses shorter than the ones of OFS that had a tail. We speculate that this might be caused by the fact that OFS deployed inside transformer captured multipath propagating acoustic wave within the transformer. The tail of the OFS waveform made it easily susceptible to interference between neighboring PD acoustic pulses. An excerpt of multiple induced PD pulses in a single power cycle when the voltage was increased to 12 kV is shown in Figure 4c. The PZT was able to capture a relatively clean waveform of multiple discernible pulses. However, the waveform picked by OFS overlapped seriously.

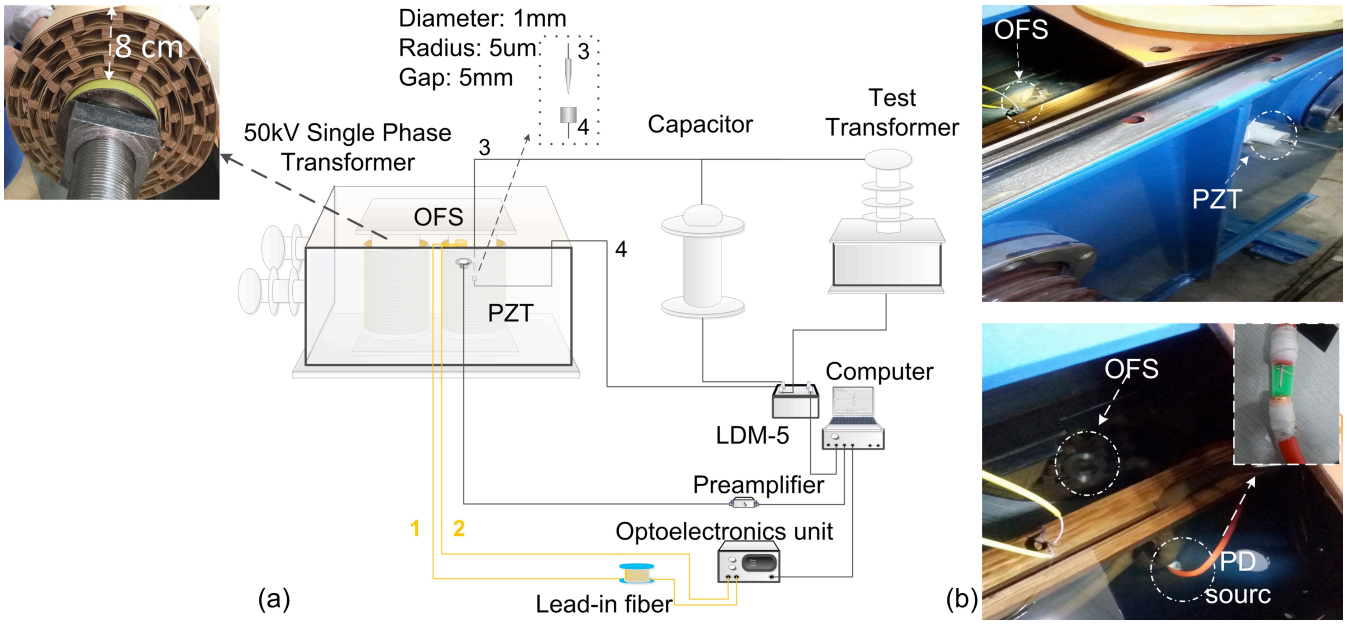

Figure 3. The experimental layout to investigate the detection efficiency of acoustic sensors when PD was induced at different locations inside the power transformer; (a) the overall experimental layout, (b) photo of deployment of OFS, PZT and PD source.

The PD source was then placed in the 3rd oil duct inside the winding, approximately 3 cm in depth, as shown in Figure 5a. In this case, the OFS showed better response to the PD than the PZT. OFS detected two wave packets around 5 ms to 8 ms and 12 ms to 15 ms, which can be clearly determined in the spectrograms obtained by applying short time Fourier transform to the temporal waveforms, as shown in Figure 5b. The spectrogram of OFS shows two hotspots at 5 ms to 8 ms and 12 ms to 15 ms lying between 60 kHz to 100 kHz, whereas the spectrogram of PZT shows a uniform power distribution of the background noise.

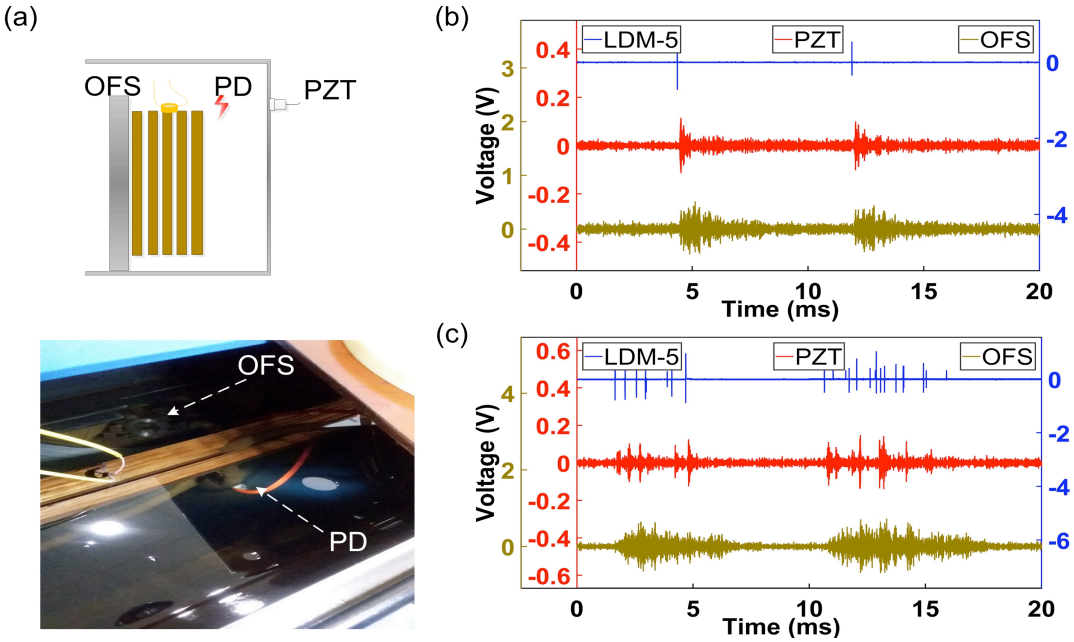

Figure 4. Detection of PD acoustic emission originated in oil outside the winding; (a) schematic and photo of experimental layout, (b) an excerpt of temporal waveform during a single power cycle under 8 kV applied voltage, (c) an excerpt of temporal waveform during a single power cycle under 12 kV applied voltage.

The above results illustrate that OFS deployed inside the transformer shows better sensitivity to PD acoustic emission induced inside the winding than the PZT mounted outside the transformer. In order to obtain a quantitative comparison, tone bursts of different frequencies induced at different locations within power transformer were used to survey the sensitivity comparison between the OFS and PZT.

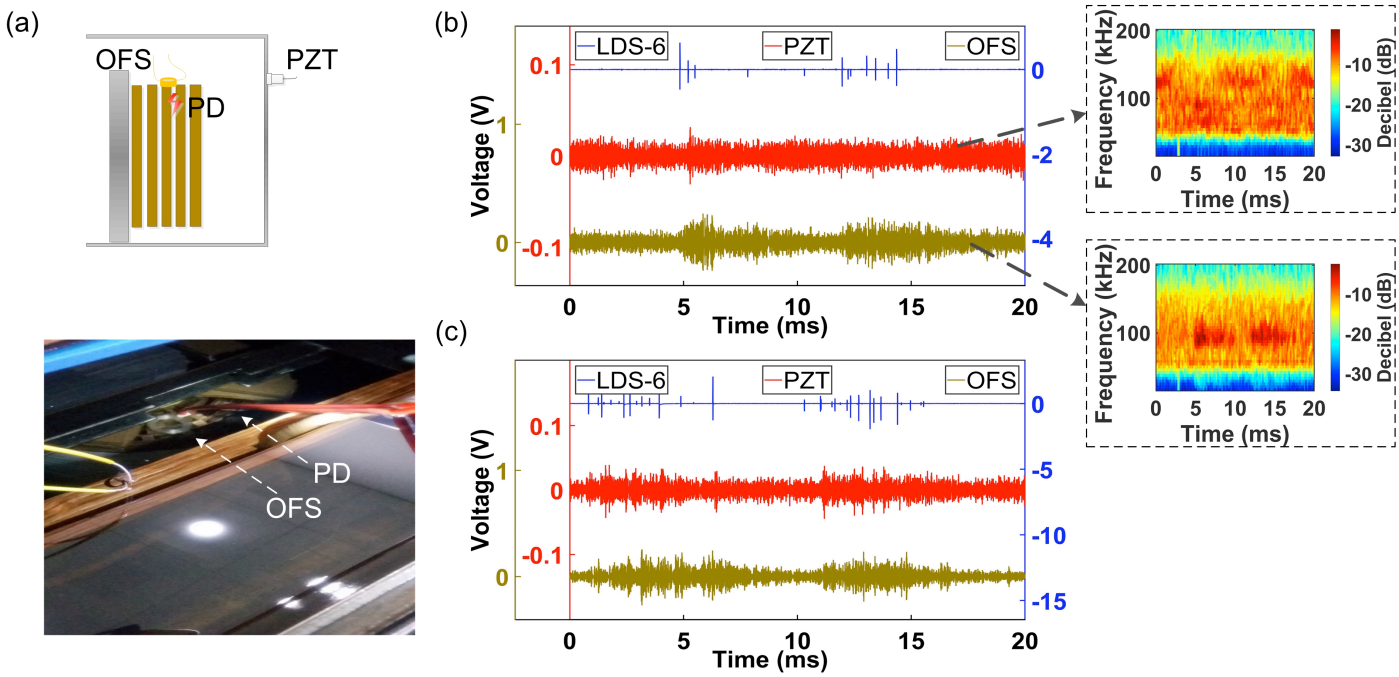

Figure 5. Detection of PD acoustic emission originated in oil duct inside the winding; (a) schematic and photo of experimental layout, (b) an excerpt of temporal waveform during a single power cycle under 10 kV applied voltage, with spectrograms of OFS and PZT shown in dashed rectangles, (c) an excerpt of temporal waveform during a single power cycle under 15 kV applied voltage.

4 SENSITIVITY GAIN SPECTRUM

The impact of tank wall on the detected signal amplitude of PZT is shown in Figure 6. Acoustic emitter was placed in oil with 9 V voltages of different frequencies applied onto it, shown in Figure 6. Two sets of signals were acquired for PZT placed inside the oil tank and outside the oil tank. A temporal waveform comparison when 130 kHz tone burst was emitted is shown in Figure 6b. The PZT deployed inside the transformer detected a 130 kHz tone burst of 6.1 $V_{peak\ to\ peak}$, whereas the PZT mounted on the outside surface of the oil tank detected a 130 kHz tone burst of 2.9 $V_{peak\ to\ peak}$. If we assume the signal amplitude is proportional to the pressure, the ratio of the signal detected by PZT on tank wall to the signal detected by PZT in oil can be taken as the transmission coefficient through the wall, as shown in black dashed curve. This result demonstrates that the transmission coefficient is frequency dependent, where it primarily stayed between 0.2 ~ 0.3 whereas increased to 0.75 at 120 kHz. An explanation will be given in section Discussion.

The acoustic emitter was placed in oil outside the winding, as shown in Figure 7a. An excerpt of detected waveforms of 150 kHz tone bursts by OFS and PZT is shown in Figure 7b, with its corresponding power spectral density of signal to noise ratio shown in Figure 7c. PZT still showed a better performance than the OFS at its resonance frequency 150 kHz. The minimum detectable applied voltages of OFS and PZT

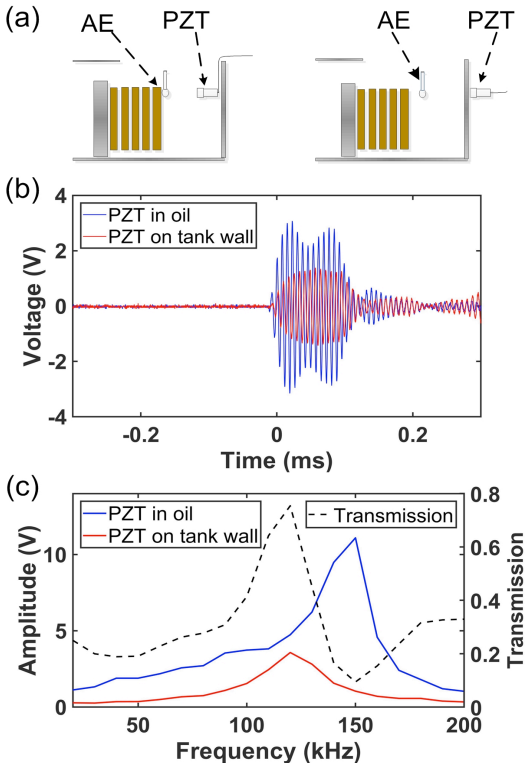

Figure 6. Tank wall impact on detection sensitivity of PZT. (a) layout schematic where PZT was placed within and outside tank. (b) an excerpt of detected waveforms of 130 kHz acoustic tone burst. (c) spectrum of signal amplitudes detected by PZT within and outside tank.

with their ratio are shown in Figure 7d. In comparison to Figure 2c, the ratio curve in black dashed line is shifted upward in decibel value, which means the performance of OFS relative to PZT was improved because the tank wall degraded the performance of the PZT.

Except the resonance frequency span from 140 kHz to 160 kHz of PZT, OFS performed better than PZT at 130 kHz ~ 200 kHz. In contrast, Figure 7f and 7g demonstrate that OFS showed better sensitivity to acoustic emissions induced 5 cm depth inside the winding than PZT. The spectrum of sensitivity comparison shown as the black dashed curve is above 0 dB at every frequency in Figure 7h.

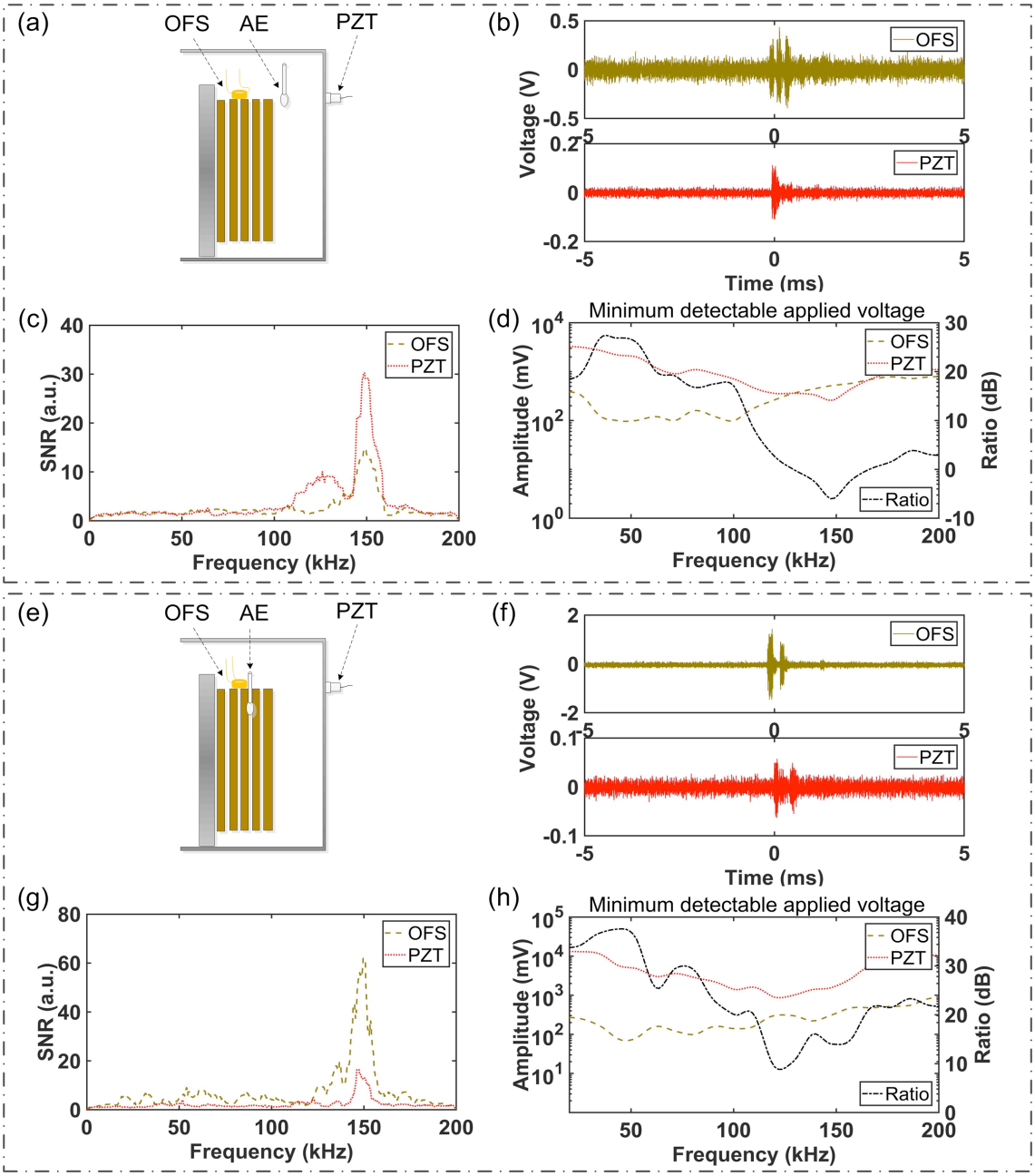

Figure 7. Sensitivity comparison between OFS and PZT to detect acoustic emissions induced at different locations. (a) layout schematic when acoustic emitter was placed in oil (b) an excerpt of detected 150 kHz temporal waveforms. (c) signal to noise ratio spectrum corresponding to (b). (d) minimum detectable applied voltage for acoustic emissions induced in oil. (e) layout schematic when acoustic emitter was placed inside the winding. (f) an excerpt of detected 150 kHz temporal waveforms. (g) signal to noise ratio spectrum corresponding to (f). (h) minimum detectable applied voltage for acoustic emissions induced inside the winding.

The maximum allowed distance between the OFS and the PD source depends on a number of factors, such as the attenuation coefficient of the insulating liquid, the PD frequency distribution and the magnitude. The minimum detectable applied voltage indicates that the proposed OFS reached its highest sensitivity of 0.1 Pa at 50 kHz. If we

assume that 1 pC PD corresponds to 0.02 Pa at 1 m away, the maximum allowed distance between the OFS and the PD source of 5 pC should be 1 m [11]. However, this distance should be much smaller, as the complicated building blocks within the power transformer attenuate or block the acoustic waves. Besides, there is still controversy over the relationship between the pressure level and the PD magnitude. Hence, whether or not a partial discharge of 5 pC will emit a 0.1 Pa acoustic emission is still under investigation. A thorough study needs to be performed in the future to understand the optimal number and locations of fiber sensors that need to be deployed within the power transformer.

5 DISCUSSION

Figure 8a shows the model that explains the frequency dependence of transmission coefficient in Figure 6c. Let the pressure fields in the 1st, 2nd, and 3rd media be denoted by E_1, E_2 and E_3. The transmission and reflection coefficients in the interfaces between media 1 and 2 and media 2 and 3 are t_{12}, r_{12}, t_{23}, and r_{23}. The transmitted field in medium 2 can be described as,

$$E_2 = t_{12}E_1 \tag{2}$$

The field in medium 2 can further transmit to medium 3, which can be described as,

$$E_3' = t_{23}E_2e^{-i\delta} \tag{3}$$

where δ is the extra added phase when wave transmits from upper interface to lower interface,

$$\delta = \frac{kd}{\cos\theta_2} \tag{4}$$

where k denotes the wavelength number, and d denotes the thickness of the tank wall. Besides, there is another wave that first reflects from the lower interface, bounces back from the upper interface and then finally transmits through the lower interface to medium 3, which can be expressed as,

$$E_3'' = t_{23}(r_{21}e^{-i\delta}r_{23}e^{-i\delta}E_2e^{-i\delta}) \tag{5}$$

The wave can also bounce forth and back for more round trips. The final transmitted field is the summation of all the above waves that can be described by,

$$E_3 = E_3' + E_3'' + E_3''' + \ldots = \frac{t_{12}t_{23}E_1e^{-i\delta}}{1 - r_{21}r_{23}e^{-i2\delta}} \tag{6}$$

The overall transmission coefficient is the ratio between E_3 and E_1, with the result shown in Figure 8b. Obviously, there is a resonance frequency span at which the transmission coefficient is high, which proves that the transmission coefficient should depend on the frequency of the acoustic wave. Nonetheless, above model is partial because acoustic wave propagating in tank wall consists of longitudinal and lateral waves so the scenario should be more complicated.

There are future improvements that can be made in order to make the fiber optic sensors truly serviceable in on-site applications. For example, fiber optic sensors are sensitive to mechanical stress, which may lead to the drifting away of fiber optic sensors from their quadrature working point and hence affect its sensitivity. In order to overcome this problem, a balanced detector can be used to passively stabilize the fiber optic sensor system as used in this research. Alternatively a feedback loop can be employed for active stabilization [26].

In summary, the results prove that fiber optic sensor deployed inside the transformer, in combination with its current applications in temperature and vibration monitoring [27], is supposed able to detect the PD acoustics inside the winding and therefore enlarge the PD acoustic detection zone.

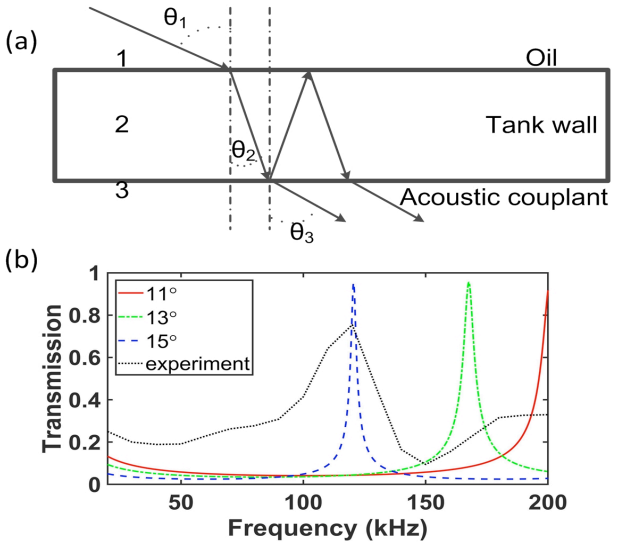

Figure 8. Transmission model and result of acoustic wave propagating through tank wall. (a) scheme of acoustic wave transmission from transformer oil through tank wall to acoustic couplant. (b) the numerical result. The solid, dot dash and dash lines show the theoretical transmission curves when the acoustic wave inputs at 11°, 13°, and 15° incidence angle. The dot line shows the experimental result in Figure 6c.

6 CONCLUSION

In this research, we used a single phase 50 kV transformer to study the benefits of using OFS to detect PD acoustic inside the power transformer. A Sagnac fiber sensor system was built and tested to survey its performance on a platform that used tone burst technique with a commercially available PZT as the benchmark. The results show that Sagnac fiber sensor system performed better at 20 kHz ~ 130 kHz, whereas the PZT performed better at 130 kHz ~ 200 kHz.

PD acoustic emissions were induced in oil outside the winding and in oil duct inside the winding. Both OFS and PZT can effectively detect the acoustic emissions originated outside the winding, whereas OFS outperformed PZT to detect the acoustic emissions originated inside the winding. Acoustic tone bursts of 20 kHz ~ 200 kHz were induced to quantitatively analyze the sensitivity comparison between OFS and PZT. PZT only outperformed OFS at 130 kHz ~ 160 kHz when tone bursts originated outside the winding. However, OFS absolutely outperformed PZT at 20 kHz ~ 200 kHz when tone bursts originated inside the winding. We envisage that OFS deployed within power transformer can effectively enlarge the detection zone of PD acoustic emission that cannot be detected by traditional method.

ACKNOWLEDGEMENT

This work is funded by National Science Foundation of China (Grant No. 51577149), State Key Laboratory of Electrical Insulation and Power Equipment (Grant No. EIPE14117), and Meidensha Corporation Japan (Grant No. 20160663). The authors would also like to show great gratitude to the help of Mr. Masayuki Sakaki, Meidensha Corporation, Japan, for his suggestion and discussion in this project.

REFERENCES

[1] S. M. Markalous, S. Tenbohlen and K. Feser, "Detection and location of partial discharges in power transformers using acoustic and electromagnetic signals," IEEE Trans. Dielectr. Electr. Insul., vol. 15, no. 6, pp. 1576-1583, 2008.

[2] M. Wang, A.J. Vandermaar and K.D. Srivastava, "Review of condition assessment of power transformers in service," IEEE Electr. Insul. Mag., vol. 18, no. 6, pp. 12-25, 2008.

[3] M. Mondal, G.B. Kumbhar and S.V. Kulkarni, "Localization of Partial Discharges inside a Transformer Winding Using a Ladder Network Constructed From Terminal Measurements," IEEE Trans. Pwr. Del., accepted, 2017, DOI: 10.1109/TPWRD.2017.2683560.

[4] N.C. Sahoo, A. Salama and R. Bartnikas R., "Trends in partial discharge pattern classification: a survey," IEEE Trans. Dielectr. Electr. Insul., vol. 12, no. 2, pp. 248-264, 2005.

[5] S. Sriram, S. Nitin, K.M.M. Prabhu and M.J. Bastiaans, "Signal denoising techniques for partial discharge measurements," IEEE Trans. Dielectr. Electr. Insul., vol. 12, no. 6, 1182-1191, 2005.

[6] E. Grossmann and K. Feser, "Sensitive online PD-measurment of onsite oil/paper insulated devices by means of optimized acoustic emission techniques," IEEE Trans. Pwr. Del., vol. 20, no. 1, pp. 158-162, 2005.

[7] Guide for the Detection and Location of Acoustic Emissions from Partial Discharges in Oil Immersed Power Transformers and Reactors, IEEE Std. C57.127, 2007.

[8] L.E. Lundgaard, "Partial discharge. XIII. Acoustic partial discharge detection-fundamental considerations," IEEE Electr. Insul., Mag., vol. 4, no.8, pp. 25-31, 1992.

[9] R. Ghosh, B. Chatterjee and S. Dalai, "A Method for the Localization of Partial Discharge Sources using Partial Discharge Pulse Information from Acoustic Emissions." IEEE Trans. Dielectr. Electr. Insul., vol. 24, no. 1, pp. 237-245, 2017.

[10] Transformer Reliability Survey, Tutorial of CIGRE A2. 37, 2011.

[11] M. Macalpine, Z. Zhao Z and L. Demokan L., "Development of a fibre-optic sensor for partial discharges in oil-filled power transformers," Electric Power Systems Research, vol. 63, no. 1, pp. 27-36, 2002.

[12] Z. Zhao, M. Macalpine and L. Demokan, "The Directionality of an Optical Fiber High-Frequency Acoustic Sensor for Partial Discharge Detection and Location," J. Lightwave Technology, vol. 18, no. 6, pp. 795-806, 2000.

[13] T.Y. Kim, K.S. Suh, H.N. Jin and T. Takada, "Acoustic monitoring of HV equipment with optical fiber sensors," IEEE Trans. Dielectr. Electr. Insul., vol. 10, no. 2, pp. 266-270, 2003.

[14] P. Rohwetter, W. Habel, G. Heidmann and P. Danniel, "Acoustic emission from DC pre-treeing discharge processes in silicone elastomer," IEEE Trans. Dielectr. Electr. Insul, vol. 22, no. 1, pp. 52-64, 2015.

[15] L. Wang, N. Fang, C. Wu, H. Qin and Z. Huang, "A fiber optic PD sensor using a balanced Sagnac interferometer and an EDFA-based DOP tunable fiber ring laser," Sensors, 2014, vol. 14, no. 5, pp. 8398-8422, 2014.

[16] S.E.U. Lima, O. Frazao, R.G. Farias, F.M. Araujo, L.A. Ferreira, J.L. Santos and V. Mirando, "Mandrel based fiber optic sensors for aocustic detection of partial discharges – a proof of concept," IEEE Trans. Pwr Del., vol. 25, no. 4, pp. 2526-2533, 2010.

[17] W. Xiaodong, L. Baoqing, R. Harry, R. Onofrio, C. Ken and F, Kenneth, "Acousto optical PD detection for transformers," IEEE Trans. Pwr. Del., vol. 21, no. 3, pp. 1068-1073, 2006.

[18] B. Dong, M. Han M, L. Sun., J. Wnag, Y. Wang, and A. Wang, "Sulfur Hexafluoride-Filled Extrinsic Fabry–PÉrot Interferometric Fiber-Optic Sensors for Partial Discharge Detection in Transformers," IEEE Photonics Technology Letters, vol. 20, no. 18, pp. 1566-1568, 2008.

[19] J. Wang, L. Min L, H. Qi and C. Wang, "An Over-Coupled Fused Coupler Based Acoustic Emission Sensor for Detecting Partial Discharges," *Symp. on Photonics and Optoelectronics*, 2012, pp. 1-4.

[20] S. Kanakambaran, R. Sarathi and B. Srinivasan, "Identification and Localization of Partial Discharge in Transformer Insulation Adopting Cross Recurrence Plot Analysis of Acoustic Signals Detected using Fiber Bragg Gratings", IEEE Trans. Dielctr. Electr. Insul., vol. 24, no. 3, pp. 1773-1780, 2017.

[21] B. Sarkar, D.K. Mishra, C. Koley, N. Roy and P. Biswas, "Intensity-Modulated Fiber Bragg Grating Sensor for Detection of Partial Discharges Inside High-Voltage Apparatus," IEEE Sensors Journal, vol. 16, no. 22, pp. 7950-7957, 2016.

[22] P. Rohwetter, R. Eisermann R and K. Krebber, "Distributed acoustic sensing: towards partial discharge monitoring," *Int. Conf. Optical Fibre Sensors (OFS24),* 2015, pp. 96341C1-96341C4.

[23] L.E. Lundgaard, "Partial discharge. XIV. Acoustic partial discharge detection-practical application," IEEE Electr. Insul. Mag., vol. 8, no. 5, pp. 34-43, 1992.

[24] H. Moller and C. Thomsen, "Electroacoustic free field measurements in ordinary room using gating techniques," B&K Application Notes 17-196, pp. 1-19.

[25] G. Luo, D. Zhang, Y. Koh, K. Ng and W. Leong, "Time frequency entropy based partial discharge extraction for nonintrusive measurement," IEEE Trans. Pwr. Del., vol. 27, no. 4, pp. 1919- 1927, 2012.

[26] T.G. Giallorenzi, J.A. Bucaro, A. Dandridge, G.H. Sigel, J.H. Cole, S.C. Rashleigh and R.G. Priest, "Optical fiber sensor technology," IEEE Trans. Microwave Theory and Techniques, vol. 30, no. 4, pp. 472-511, 1982.

[27] K. Peter, W. Lutang and C. Maria, "A comprehensive condition monitoring solution for the transformer," *IEEE Int. Conf. on Electric Machines,* 2012, pp. 1520-1525.

Sen Qian is currently a PhD student in Electrical Engineering Department of Xi'an Jiaotong University, Shaanxi, China. His research interests are power equipment monitoring, fiber optic sensor, fiber optics, dielectric liquid and natural ester insulating oil.

Hao Chen is currently a PhD student in Electrical Engineering Department of Xi'an Jiaotong University, Shaanxi, China. His research interests are power equipment monitoring, fiber optic sensor, fiber optics, photonic crystal.

Yang Xu(M'05) is now a professor at Xi'an Jiaotong University. His research interest lies in partial discharge detection for cables, partial discharge detection using optical fiber sensor, and natural ester oil-paper insulation system.

Lei Su is a lecturer with the School of Engineering and Materials Science at Queen Mary University of London and his current research is mainly concerned with optical sensors for diagnosis, imaging and monitoring.